

An Efficient Stochastic Optimization Method for Global Placement in VLSI Problem

Yi-Shuang Yue^{2,1}, Yu-Hong Dai^{1,2}, Haijun Yu^{1,2*}

¹LSEC & ICMSEC, Academy of Mathematics and Systems Science, Chinese Academy of Sciences, No. 55 Zhongguancun East Road, Haidian District, 100190, Beijing, China.

²School of Mathematical Sciences, University of Chinese Academy of Sciences, Beijing, 100049, China.

*Corresponding author(s). E-mail(s): hyu@lsec.cc.ac.cn;
Contributing authors: yueyishuang@amss.ac.cn; dyh@lsec.cc.ac.cn;

Abstract

The placement problem in very large-scale integration (VLSI) is a critical step in chip design, the goal of which is to optimize the wirelength of circuit components within a confined area while adhering to non-overlapping constraints. Most analytical placement models often rely on smooth approximations, thereby sacrificing the accuracy of wirelength estimation. To mitigate these inaccuracies, this paper introduces a novel approach that directly optimizes the original nonsmooth wirelength and proposes an innovative penalty model tailored for the global placement problem. Specifically, we transform the non-overlapping constraints into rectified linear penalty functions, allowing for a more precise formulation of the problem. Notably, we reformulate the resultant optimization problem into an equivalent framework resembling deep neural network training. Leveraging automatic differentiation techniques from deep learning, we efficiently compute the subgradient of the objective function, thus facilitating the application of stochastic subgradient methods to solve the model. To enhance the algorithm's performance, several advanced techniques are further introduced, leading to significant improvements in both efficiency and solution quality. Numerical experiments conducted on GSRC benchmark circuits demonstrate that our proposed model and algorithm achieve significant reductions in wirelength while effectively eliminating overlaps, highlighting its potential as a transformative advancement for large-scale VLSI placement.

Keywords: VLSI placement problem, stochastic subgradient algorithm, nonsmooth nonconvex optimization, penalty method, rectified linear deep neural networks

1 Introduction

Circuit placement is a fundamental and critical stage in the physical design of very large-scale integrated circuits (VLSI). Its primary goal is to determine the specific locations of physical units within a predefined placement area, ensuring device non-overlapping constraints are satisfied while optimizing key performance metrics such as wirelength, delay, and area utilization [1]. The quality of circuit placement has a profound impact on subsequent design stages, including post-placement optimization and routing, directly influencing circuit performance, power consumption, chip area, manufacturing cost, signal integrity, and so on. The placement problem is a typical NP-hard problem [2], necessitating the development of advanced algorithms to address its complexity. Existing solutions can broadly be classified into three categories: simulated annealing [3], partitioning [4], and analytical methods [5]. The simulated annealing method emulates the physical annealing process, and gradually optimizes the placement by randomly swapping, rotating, or moving modules, assessing the effects of these changes to find the global optimum. Partitioning methods address the placement problem by recursively dividing large instances—comprising net lists and placement regions into smaller sub-problems. Once the instance is sufficiently reduced, efficient local optimization algorithms are applied to achieve high-quality placements within each partition [6]. Analytical methods leverage linear or nonlinear programming techniques to obtain optimal or near-optimal solutions for the placement problem. By modeling placement objectives and constraints mathematically, analytical approaches have emerged as a dominant paradigm for solving large-scale VLSI placement problems, offering exceptional accuracy and scalability [7].

The placement problem can rigorously be formulated as a constrained optimization problem, where the primary objective is to minimize the half-perimeter wirelength (HPWL) while satisfying non-overlapping constraints for physical units. Different methodologies for approximating and optimizing wirelength have led to the emergence of two major categories of placement models: smooth models and nonsmooth models. The smooth model approximates the original nonsmooth HPWL using continuously differentiable objective functions, such as L_p norms [8], the log-sum-exp functions [9] and weighted average model [10]. To address the overlap constraints, smoothing techniques like the Gaussian equation [11] and Helmholtz equation [8] are often employed. These techniques relax the problem by transforming the original nonsmooth optimization into a smooth nonlinear programming problem. Smooth models are widely adopted in modern placement solvers, which incorporate penalty methods, conjugate gradient methods, and Nesterov’s accelerated techniques for efficient optimization. The nonsmooth optimization models directly address the original nonsmooth HPWL. The HPWL objective function inherently involves absolute values, which introduce discontinuities and nondifferentiable points, making it a challenging optimization landscape. To overcome these difficulties, researchers have developed specialized algorithms tailored for nonsmooth structures, such as the conjugate subgradient method [12] and the mixed-variable optimization [13], which are more adept at handling discontinuities caused by absolute values.

Existing smooth models, while exhibiting high computational efficiency, suffer from limitations in accuracy due to their reliance on smooth approximations. This limitation

becomes particularly pronounced in large-scale designs, where approximation errors can accumulate and lead to suboptimal solutions and additional adjustment costs. On the other hand, nonsmooth models can accurately represent the original structure of the HPWL, but their non-differentiable objective functions and constraints make conventional gradient-based optimization methods inapplicable. Therefore, the core motivation of our research is to design a solution algorithm that preserves the accuracy of HPWL representation while handling nondifferentiable points and maintaining high computational efficiency.

In this paper, we propose a promising nonsmooth optimization model for VLSI global placement based on the absolute wirelength function and the penalty function calculated by the overlap between cells and the distance between cells and boundaries. In this model, the objective function is defined as the HPWL wirelength function, and the non-overlapping constraint is characterized by the piecewise linear hat function related to the overlap of the elements, which is free of gradient vanishing and gradient exploding if gradient methods are used. Due to the nonconvex and nonsmooth properties of the problem, we design a stochastic subgradient descent operator splitting algorithm to solve it. The solution procedure is formulated as a neural net training problem and is implemented using the deep learning toolkit PyTorch [14]. Several dedicated techniques are further introduced, including degree-weighted sampling based on hypergraph, adaptive parameter updating, and random disturbance, to improve the performance and placement effect of the algorithm. In addition, we also propose an alternate optimization legalization algorithm by combining wirelength optimization and de-overlap technique, which eliminates overlap while maintaining the advantage of short wirelength. We conducted numerical experiments to compare our proposed algorithm with the benchmark provided by GSRC [15]. The results demonstrate significant improvements in wirelength reduction and overlap elimination, thereby highlighting the advantages and potential of our proposed model and algorithms in solving VLSI placement problems.

The rest of this article is organized as follows. In the second section, we first present the mathematical model for the placement problem, followed by the derivation of the corresponding penalty function model. The third section is devoted to the stochastic subgradient method to optimize the nonsmooth penalty model, and the fourth section presents experimental results on the GSRC benchmark. Finally, the fifth section offers a summary of the article.

2 The placement problem and mathematical models

2.1 The problem definition

A VLSI circuit board can be modeled as a hypergraph $H(V, E)$, where $V = \{v_1, v_2, \dots, v_n\}$ denotes the set of cells, each cell $v_i = (x_i, y_i)$ represents a physical component of the circuit, and $E = \{e_1, \dots, e_m\}$ denotes the set of nets. Each net $e_k \in E$ is a subset of V , corresponding to a group of cells that are electrically interconnected.

Each cell $v_i \in V$, for $i = 1, \dots, n$, is modeled as a rectangular block defined by its width w_i and height h_i . The placement region for these cells is a designated rectangular

area bounded by the coordinates $(0,0)$ at the lower left corner and (W,H) at the upper right corner.

The objective of the VLSI placement problem is to determine the optimal positions for the cells within the placement region such that the total wirelength, measured as the sum of the lengths of the nets connecting the cells, is minimized. Additionally, the placement must satisfy the constraint that no two cells overlap within the designated area. A mathematical formulation of the VLSI global placement problem for mixed cells is described as follows [16]:

$$\min_{\mathbf{x}} \text{HPWL}(\mathbf{x}, \mathbf{y}) := \sum_{e \in E} \left(\max_{(v_i, v_j) \in e} |x_i - x_j| + \max_{(v_i, v_j) \in e} |y_i - y_j| \right) \quad (1)$$

$$\text{s.t.} \quad |x_i - x_j| \geq \frac{w_i + w_j}{2} \text{ or } |y_i - y_j| \geq \frac{h_i + h_j}{2}, \quad \forall (v_i, v_j) \in e, \quad (2)$$

$$\frac{w_i}{2} \leq x_i \leq W - \frac{w_i}{2} \text{ and } \frac{h_i}{2} \leq y_i \leq H - \frac{h_i}{2}, \quad \forall (x_i, y_i) \in V. \quad (3)$$

Here, $\mathbf{x} = (x_1, \dots, x_n)$, $\mathbf{y} = (y_1, \dots, y_n)$, $\mathbf{X} = \{\mathbf{x}, \mathbf{y}\}$. HPWL stands for the half-perimeter wirelength. The objective function and constraints specified in the problem (1)–(3) are nonconvex and nonsmooth, making it a challenging optimization problem. To overcome these difficulties, a penalty method is employed to relax the constraints, enabling the reformulation and transformation of the problem into a neural network framework. The reformulated problem is then optimized using advanced deep learning techniques.

2.2 A rectified linear penalty method

To enforce the boundary condition, we adopt the following penalty terms:

$$\begin{aligned} \ell_b(x_i, y_i) := & \text{ReLU}\left(\frac{w_i}{2} - x_i\right) + \text{ReLU}(x_i - w_i^+) \\ & + \text{ReLU}\left(\frac{h_i}{2} - y_i\right) + \text{ReLU}(y_i - h_i^+), \end{aligned} \quad (4)$$

where $w_i^+ = W - w_i/2$, $h_i^+ = H - h_i/2$, $\text{ReLU}(x) := \max(0, x)$. To enforce the nonoverlap constraints, a straightforward approach introduces the following penalty function:

$$\ell_x(x_i, x_j) := \text{ReLU}\left(\frac{w_i + w_j}{2} + x_i - x_j\right) \times \text{ReLU}\left(\frac{w_i + w_j}{2} + x_j - x_i\right), \quad (5)$$

$$\ell_y(y_i, y_j) := \text{ReLU}\left(\frac{h_i + h_j}{2} + y_i - y_j\right) \times \text{ReLU}\left(\frac{h_i + h_j}{2} + y_j - y_i\right) \quad (6)$$

to formulate a penalty problem as

$$\min_{\mathbf{x}} \left\{ \text{HPWL}(\mathbf{x}, \mathbf{y}) + \sum_{(x_i, y_i) \in V} \gamma_i \ell_b(x_i, y_i) + \sum_{i < j} \gamma_{ij} \ell_x(x_i, x_j) \ell_y(y_i, y_j) \right\}. \quad (7)$$

However, due to the peculiarities of overlapping penalty terms (the subderivative of $\ell_x \ell_y$ can be very close to 0), this penalty function model may encounter the problem of gradient vanishing during optimization.

Alternative approaches exist for constructing the overlap penalty. In [12], the placement area is uniformly partitioned into a grid of non-overlapping bins, and the squared difference between the overlapping cell area and the bin area is used as the penalty term. A recent work [13], on the other hand, chooses the square root of the overlapping area as the penalty term. However, both of these methods suffer from the gradient vanishing issue, which limits their effectiveness in optimization.

To remove the deficiency of the nonoverlap penalty, we need to use different penalties for $\ell_x \ell_y$ in (7). We note that (5) and (6) are quadratic polynomials when (3) is not satisfied, which leads to the fact that the derivatives can be very small. To remedy this, we propose the following two-dimensional piecewise linear hat function to replace the piecewise quadratic function $\ell_x \ell_y$:

$$\varphi_{r,t}(x, y) = \begin{cases} 0, & \text{if } |x| \geq r \text{ or } |y| \geq t; \\ 1 - \frac{|x|}{r}, & \text{if } \frac{|y|}{t} \leq \frac{|x|}{r} < 1; \\ 1 - \frac{|y|}{t}, & \text{if } \frac{|x|}{r} < \frac{|y|}{t} < 1. \end{cases} \quad (8)$$

Then, a two-dimensional penalty for pair-wise overlap can be constructed as

$$\ell_{xy}(x_i, y_i, x_j, y_j) = \varphi_{w_{ij}, h_{ij}}(x_i - x_j, y_i - y_j), \quad w_{ij} = \frac{w_i + w_j}{2}, \quad h_{ij} = \frac{h_i + h_j}{2}. \quad (9)$$

The new penalty problem can be modeled as

$$\min_{\mathbf{x}} \left\{ \text{HPWL}(\mathbf{x}, \mathbf{y}) + \sum_{(x_i, y_i) \in V} \gamma_i \ell_b(x_i, y_i) + \sum_{i < j} \gamma_{ij} \ell_{xy}(x_i, y_i, x_j, y_j) \right\}. \quad (10)$$

Remark 1. We can also replace $1 - |x|/r$ by $(rt - t|x|)$, and replace $1 - |y|/t$ by $(rt - r|y|)$, in (8), but our numerical experiments show that they lead to similar results.

We note that it can be proved that a one-dimensional rectified linear penalty is exact. However, the two-dimensional rectified linear penalty for pairwise overlap is not. Let us consider a case presented in Figure 1. In the left plot, the derivatives with respect to the positions of A and B cells are zeros. But in the right plot, a directional derivative of the pairwise non-overlapping penalty with respect to the position of B can be infinitely close to 0, e.g. the directional derivative along a direction d which is

a small perturbation to the x -direction. Therefore, if the HPWL has a finite nonzero gradient along this direction, the non-overlapping constraint will be violated. Thus, the penalty is not exact.

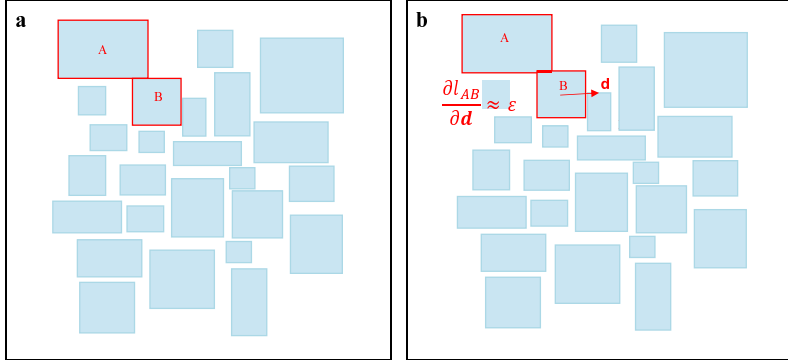


Fig. 1 **a)** A placement corresponding to a local minimum point of the original problem (1)-(3); **b)** a small perturbation of the placement **a**, where along certain directions the HPWL has a finite decrease but the directional derivative of the overlap penalty may be arbitrarily small. Therefore, the objective function of the penalty model (10) will decrease along this direction, and the non-overlapping constraint will be violated, no matter how large the penalty constant are. In this case, the local minimum of model (10) will not be a local minimum of the original problem.

Although the new penalty function model is not exact, we can prove that the amplitude of nonzero gradients of the penalty term has a lower and an upper bound (see Theorem 1), so that the problem of gradient vanishing and gradient exploding can be avoided and better optimization results can be obtained.

Theorem 1. *The l^p norm of nonzero gradients of the penalty term $\sum_{(x_i, y_i) \in V} \gamma_i \ell_b(x_i, y_i) + \sum_{i < j} \gamma_{ij} \ell_{xy}(x_i, y_i, x_j, y_j)$ has a lower bound and an upper bound.*

Proof. We consider the l^1 norm. The cases $p \neq 1$ are similar. The l^1 norm of the nonzero subgradient of $\ell_b(x_i, y_i) := \text{ReLU}(\frac{w_i}{2} - x_i) + \text{ReLU}(x_i - w_i^+) + \text{ReLU}(\frac{h_i}{2} - y_i) + \text{ReLU}(y_i - h_i^+)$ satisfies

$$1 \leq \|\partial \ell_b(x, y)\|_1 \leq 2.$$

The l^1 norm of the nonzero subgradient of $\ell_{xy}(x_i, y_i, x_j, y_j)$ defined in (9) is:

$$\|\partial \ell_{xy}(x_i, y_i, x_j, y_j)\|_1 = \begin{cases} \frac{1}{w_{ij}}, & \frac{|y_i - y_j|}{h_{ij}} \leq \frac{|x_i - x_j|}{w_{ij}} < 1, \\ \frac{1}{h_{ij}}, & \frac{|x_i - x_j|}{w_{ij}} < \frac{|y_i - y_j|}{h_{ij}} < 1. \end{cases}$$

Thus it is clear that the nonzero gradient norm of the penalty term $\sum_{(x_i, y_i) \in V} \gamma_i \ell_b(x_i, y_i) + \sum_{i < j} \gamma_{ij} \ell_{xy}(x_i, y_i, x_j, y_j)$ has a lower and an upper bound. \square

Now, we show that the new penalty model (10) can be transformed into a deep ReLU network. First, for absolute value functions, we can reformulate it as

$$|x| = \text{ReLU}(x) + \text{ReLU}(-x).$$

The maximum of two values can be expressed as

$$\max(a, b) = \text{ReLU}(a - b) + b = \text{ReLU}(b - a) + a, \quad (11)$$

and the maximum of 4 values can be expressed as a composition of two layers of ReLU functions by (11) and the following identity

$$\max(a, b, c, d) = \max(\max(a, b), \max(c, d)).$$

Similarly, the maximum of 2^n values can be expressed as a composition of n layers of ReLU functions. So the HPWL defined in (1) can be formulated into a deep ReLU neural network with $\lceil \log M \rceil + 1$ ReLU layers, where $M = \max_{e \in E} \{\#e\}$. Here $\lceil x \rceil$ represents the smallest integer that no smaller than x , and $\#e$ denotes the number of elements in a net e . The boundary penalty (4) is already formulated as a network of one ReLU layer. The pairwise penalty (8) can be formulated as a neural network of 3 ReLU layers. In summary, the new model (10) can be formulated as a deep neural network with $\max\{\lceil \log M \rceil + 1, 3\}$ ReLU layers.

2.3 Analogy to deep learning

Both analytic placement and training neural nets are essentially solving nonlinear optimization problems. In the context of supervised learning, neural network training involves feeding input data, consisting of feature vectors and corresponding labels, into the network [17]. The network computes a loss function based on the predicted and actual values, and optimization algorithms are employed to iteratively update the network parameters using gradients. This process continues until the loss is minimized and the network accurately predicts the labels for the given data. In our placement problem, we directly optimize the objective function composed of wirelength and overlap boundary constraint penalties, continuously updating the block positions until the objective function is optimized, which can be reviewed as a reinforcement learning approach. Furthermore, a direct analogy can be drawn between the placement problem and neural network training, see Fig. 2. The input data instance is replaced with net information, the feature vector represents key information such as net connection and block information, the label is set to an empty set, and the block positions $\{(x_i, y_i)\}$ correspond to net parameters. The loss is defined as our objective functions (10), and the parameters, i.e., the block positions, are adjusted throughout the training process to minimize the loss function. By establishing this one-to-one mapping, the placement problem is effectively reformulated as a neural net training problem. This transformation allows the use of deep learning techniques to solve placement problems, using forward propagation to compute objectives and backward propagation to calculate gradients, thereby enabling the implementation of efficient optimization strategies.

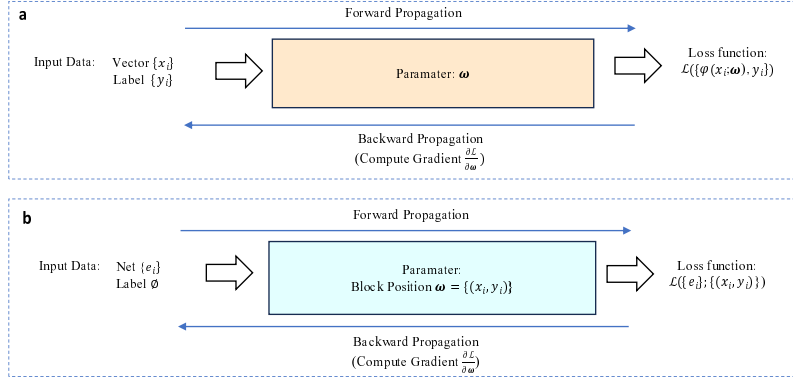


Fig. 2 Analogy between neural network training and placement problem training. The top plot (a) illustrates a supervised learning process, and the bottom plot (b) illustrates our method, which is a reinforcement learning approach. Both of them utilize back propagation to solve the network training problem.

3 The stochastic algorithm

3.1 Random batch split method

In the last section, the original constrained optimization problem was reformulated into a unconstrained optimization problem using penalty methods. Due to the nonsmooth and nonconvex nature of the problem, traditional optimization techniques may struggle to efficiently identify solutions close to the global minimum. Therefore, we will employ a stochastic subgradient method to solve this nonsmooth optimization problem. The objectives of the models are formulated as follows:

$$J(V) = \sum_{e \in E} \ell_e + \sum_{(x_i, y_i) \in V} \gamma_i \ell_b(x_i, y_i) + \sum_{i < j} \gamma_{ij} \ell_{xy}(x_i, y_i, x_j, y_j). \quad (12)$$

In this study, we employ the operator splitting method [18] to optimize the interaction function in placement problems. This method improves efficiency and precision by decomposing the interaction function into two components—a short-range component

$$J_1 = \sum_{(x_i, y_i) \in V} \gamma_i \ell_b(x_i, y_i) + \sum_{i < j} \gamma_{ij} \ell_{xy}(x_i, y_i, x_j, y_j),$$

and a long-range component

$$J_2 = \sum_{e \in E} \ell_e.$$

The short-range component J_1 mainly solves the loss caused by boundary and overlap, which is only valid when the unit has overlap or exceeds the boundary, so the calculation involving this component can be completed quickly, the computational complexity can be reduced from $O(N^2)$ to $O(N)$ by filtering items that only overlap with the block through meshing. The remote component J_2 is the distance loss, the

loss function is bounded, and the calculation amount can be effectively reduced using mini-batch technology.

In the subsequent sections, we provide a detailed explanation of the algorithm’s implementation, focusing on how further techniques are combined to optimize the placement problem effectively.

3.1.1 Adaptive parameter adjustment

In penalty-based optimization problems, selecting appropriate parameter values is crucial. Parameters that are too small fail to ensure the accuracy of the solution, while excessively large parameters can lead to numerical instability and make the optimization algorithm overly sensitive, thereby hindering convergence to a stable solution. Therefore, careful consideration is required in determining the parameter values.

In this paper, we adopted an adaptive parameter updating strategy that dynamically adjusts parameter values based on their contributions to the loss function. This approach effectively guides the search process to focus more on the current part that needs to be improved. At first, we initialize the parameter by a uniform value γ_0 , then the following formula is used to calculate the parameter at each step of iteration [12] [19]:

$$\tilde{\gamma}_i = \begin{cases} \left\lceil \max \left(\frac{\partial(\ell_e)_i}{\partial(\ell_b(x_i, y_i))_i} \right) \right\rceil, & \text{if } \partial(\ell_b(x_i, y_i))_i \neq 0, \\ \gamma_0, & \text{if } \partial(\ell_b(x_i, y_i))_i = 0. \end{cases} \quad (13)$$

$$\tilde{\gamma}_{ij} = \begin{cases} \left\lceil \max \left(\frac{\partial(\ell_e)_i}{\partial(\ell_{xy}(x_i, y_i, x_j, y_j))_i} \right) \right\rceil, & \text{if } \partial(\ell_{xy}(x_i, y_i, x_j, y_j))_i \neq 0, \\ \gamma_0, & \text{if } \partial(\ell_{xy}(x_i, y_i, x_j, y_j))_i = 0. \end{cases} \quad (14)$$

Here $\partial(\ell_e)_i$ represents the generalized derivative of ℓ_e with respect to (x_i, y_i) , with similar definitions applying to $\partial(\ell_b(x_i, y_i))_i$ and $\partial(\ell_{xy}(x_i, y_i, x_j, y_j))_i$. The expression $\frac{\partial(\ell_e)_i}{\partial(\ell_{xy}(x_i, y_i, x_j, y_j))_i}$ represents element-wise division, *max* denotes taking the maximum over all terms. The notation $\lceil \cdot \rceil$ represents the ceiling function. Experimental results demonstrate that the use of rounding via the ceiling function significantly accelerates the algorithm, enhancing both computational efficiency and solution quality.

3.1.2 Degree weighted sampling based on hypergraph

Experimental results demonstrate that the use of rounding via the ceiling function significantly accelerates the algorithm, enhancing both computational efficiency and solution quality. To improve the efficiency further, we employ a degree-weighted sampling method based on hypergraph to train the net in batches. In this method, each net is represented as a vertex in the hypergraph, and an edge is established between two vertices if the corresponding nets share a common block.

Using this topological structure, the “degree” of each net vertex is defined as the number of connections it has with other vertices, reflecting its connectivity density [20]. Higher-degree nets are more closely related to other nets, and their optimization is typically more challenging. To prioritize the optimization of critical nets, we adopt

a sampling strategy that gives higher selection probability to nets with larger degrees. Specifically, for the net set $E = \{e_1, \dots, e_m\}$, if the degree of the net e_i is d_i , the sampled probability p_i of net e_i is calculated as follows:

$$p_i = \frac{e^{d_i/T}}{\sum_{j=1}^m e^{d_j/T}}, \quad (15)$$

where T is a constant parameter resembling temperature. With this weighted sampling strategy, we can not only improve the efficiency of training but also ensure that sufficient attention is paid to the optimization of key nets, thus accelerating the solving process of the overall placement problem while maintaining performance. The algorithm of degree weighted sampling is as follows (Algorithm1):

Algorithm 1 Degree weighted sampling

- 1: Create a mapping for each terminal to record which nets contain the terminal.
 - 2: Build the hypergraph of mapping and calculate the degree of the vertices.
 - 3: Calculate the sampling probability for each net using formula (15).
-

3.1.3 Mean field force

To achieve a more compact arrangement of blocks, a regularization term which known as “mean field force” [21], is incorporated into the objective function. This term is designed to reduce the distance between each block and the center of the placement region, thereby promoting tighter block placement. The regularization term is defined as:

$$\mathcal{E}_{mean} = \sum_{v_i \in V} \alpha \|(x_i, y_i) - (x_{mean}, y_{mean})\|_2^2.$$

Here α is the force parameter. (x_{mean}, y_{mean}) represents the average position of all blocks. By incorporating this regularization term into the optimization process, the arrangement of blocks becomes more balanced, thereby reducing the overall placement area and significantly decreasing the total wirelength. Moreover, the inclusion of this term accelerates convergence to a stable configuration and mitigates the risk of being trapped in local minima.

3.1.4 Incorporation of random disturbance

One of the main challenges of nonconvex optimization problems is the potential to become trapped in local minima. To address this issue and promote a more comprehensive exploration of the solution space, we have integrated a stochastic process into our algorithm. These stochastic components are designed to introduce randomness, thereby enhancing the algorithm’s ability to escape local minima. The key stochastic components are implemented as follows:

1. **Random initialization:** Initial coordinates (x_i^0, y_i^0) are randomly sampled from a specified range to enhance the diversity of initial configurations.

2. **Incorporation of random forcing:** By adding some Gaussian random disturbances to the gradient, noise is introduced into the optimization process of the algorithm, which can effectively help the optimization to escape local minima [22]. The algorithm for adding random perturbations can be summarized as Algorithm 2:

Algorithm 2 Gaussian random disturbance

- 1: **for** Step k **do**
- 2: Calculate the subgradient \mathbf{g} of loss function.
- 3: Generate a Gaussian random vector $\boldsymbol{\eta}$ with the same shape as the subgradient.
- 4: Calculate the perturbation coefficient by $\epsilon = 0.2/k^3$.
- 5: Add perturbation and update subgradient by:

$$\mathbf{g} = \mathbf{g} + \epsilon \|\mathbf{g}\| \boldsymbol{\eta}$$

- 6: **end for**
-

By incorporating these stochastic ingredients, the algorithm has a better efficiency in exploring the solution space, enhancing the likelihood of identifying globally optimal or near-optimal solutions.

3.2 The overall random batch split algorithm

Combining all the above details, our algorithm can be summarized as Algorithm 3, which we refer to as random batch splitting method (RBSM).

In the position update phase, distance loss and penalty are calculated separately, enabling two targeted position updates. This approach allows for more effective and focused adjustments to overlap and wirelength. After each update of γ , the model is trained until the local minimum is reached. Based on experimental results, it was observed that stochastic gradient descent (SGD) typically converges to a local minimum within 25 iterations. Therefore, a fixed iteration count of 25 is used instead of a variable stopping criterion. To update the learning rate, we adopt the cosine annealing schedule from PyTorch, which gradually reduces the learning rate over iterations. This scheduling strategy helps improve convergence stability and avoid oscillations near local minima. At last, we adopted a practical and reasonable termination criterion commonly used in analytical placement methods, which is to stop the algorithm when the target HPWL satisfies condition $\left| \frac{\text{HPWL}(x^k, y^k)}{\text{HPWL}(x^{k+1}, y^{k+1})} - 1 \right| < \epsilon_{\text{hpwl}}$ and the overlap ratio meets $\text{ratio}_{\text{overlap}} < \epsilon_{\text{overlap}} = 2\%$.

3.3 Alternate optimization legalization

Due to the fact that the penalty is not exact, overlaps cannot be entirely eliminated during the global placement stage, thus further de-overlapping is required in the legalization phase. Typically, traditional legalization focuses solely on eliminating overlaps, which might lead to a significant increase in wirelength. To address this, we use a strategy that alternates between optimizing overlap and minimizing distance loss. This method simultaneously reduces overlap and prevents significant increases in wirelength. Initially, the algorithm calculates distance loss and updates positions to reduce

Algorithm 3 RBSM for function (12)

```
1: Input:  $iter_{max}$ , tolerance  $\epsilon_{hpwl} = 0.0001$ ,  $\epsilon_{overlap} = 2\%$ ;  
2: Output: Optimal placement position  $(x^*, y^*)$ ;  
3:  $k \leftarrow 0$   
4: while  $k < iter_{max}$  do  
5:   Split  $J(V)$  into two parts: distance term  $J_1$  and penalty term  $J_2$ .  
6:   Initialize  $(\mathbf{x}^0, \mathbf{y}^0)$  randomly and set initial learning rate  $lr_0 = 0.1$ .  
7:   Calculate  $\gamma_i^k$  and  $\gamma_{ij}^k$  using equations (13), (14)  
8:   for  $step = 1$  to 25 do  
9:     Sample from  $E$  by Algorithm 1 to obtain batch  $E_q$ .  
10:    for batch  $E_q$  do  
11:      Compute distance loss  $J_1$  and get subgradient via automatic differentiation.  
12:      Add random perturbations by Algorithm 2 and update positions by gradient  
method:  $(\mathbf{x}, \mathbf{y}) \leftarrow (\mathbf{x}, \mathbf{y}) + lr * (\mathbf{g} + \epsilon \|\mathbf{g}\| \eta)$ .  
13:      Compute penalty term  $J_2$  and get subgradient via automatic differentiation.  
14:      Add random perturbations to update positions by gradient method similarly.  
15:    end for  
16:  end for  
17:  Get  $(\mathbf{x}^{k+1}, \mathbf{y}^{k+1})$  after all steps.  
18:   $lr \leftarrow lr_0 \times \left(1 + \cos\left(\frac{\pi \times k}{iter_{max}}\right)\right) / 1$ .  
19:  if  $\left|\frac{HPWL(x^{k-1}, y^k)}{HPWL(x^{k+1}, y^{k+1})} - 1\right| < \epsilon_{hpwl}$  and  $ratio_{overlap} < \epsilon_{overlap}$  then  
20:    Stop and return  $(\mathbf{x}^*, \mathbf{y}^*) = (\mathbf{x}^k, \mathbf{y}^k)$   
21:  end if  
22:   $k \leftarrow k + 1$   
23: end while
```

the distance between components. It then assesses the overlap penalty, calculates gradients via automatic differentiation, and updates positions based on calculated steps to minimize overlaps. This process of alternating updates continues until overlaps are eliminated and distance stabilizations are achieved. We note that for the rectified linear penalty, the legalization of non-overlapping can be made exact in one step for individual pairwise constraint, if these constraints are not coupled. But, since there might exist coupled non-overlapping constraints, we use multiple rounds of legalization iteration.

The specific steps are given in Alg. 4.

4 Numerical experiments

4.1 Experimental setup

In this section, we present a series of numerical experiments to assess the performance of three different methods: gradient descent (GD) [23], ADAM [24], and RBSM. The evaluation is conducted using the GSRC benchmarks which are widely used to test and evaluate electronic design automation tools and algorithms. The codes were written in Python and run on a standard PC with an i9-13980HX microprocessor and 32GB of memory.

4.2 Results analysis

We implement the RBSM method, GD method, and ADAM method in Python. The GD method only uses the built-in SGD subroutine of Torch for optimization, while the ADAM method is combined with a series of enhanced techniques we used, including parameter updates, mean field force, and weighted sampling. This is to compare the optimization algorithm and enhanced techniques from two perspectives. In the RBSM and ADAM methods, the parameters are set to identical values: average field force coefficient $\alpha = 5$, batch size is $1/5$ of the total number of nets, and the initial value of parameter γ is 1000. In the GD method, γ is always set to a constant of 1000. We verify the feasibility and performance of the proposed algorithm by GSRC plane planning benchmarks. The final GSRC graphic design results were used as a test. We compared the wirelength and overlap of the different methods, as well as the visual effects of the placement (see Appendix). Table 1 shows the experimental data of GSRC and the results of different algorithms, and Table 2 shows the placement results and legalization results of different algorithms in the benchmark test.

Through the experimental results, we can observe the following points:

1. The proposed placement algorithm effectively reduces overlap while significantly minimizing wirelength. This dual improvement demonstrates the method's strong potential, as conventional placement algorithms often struggle to simultaneously

Algorithm 4 Legalization Algorithm

```

1: for  $k$  from 1 to 10 do
2:   Calculate distance loss by  $\ell_e := \max_{(v_i^k, v_j^k) \in e} |x_i^k - x_j^k| + \max_{(v_i^k, v_j^k) \in e} |y_i^k - y_j^k|$ 
3:   Update positions by gradient descent method.
4:   for block  $I(\text{position}(x_i, y_i))$  in  $V$  do
5:     if block  $J(\text{position}(x_j, y_j))$  overlaps  $I$  then
6:       Get subgradient  $g_i$  of  $\ell_{xy}$  for  $(x_i, y_i)$  by automatic differentiation.
7:       Calculate step by
           
$$\alpha_i = \begin{cases} r_{ij} - |x_i - x_j| & \text{if } \frac{\partial \ell_{xy}}{\partial x} \neq 0, \\ t_{ij} - |y_i - y_j| & \text{if } \frac{\partial \ell_{xy}}{\partial y} \neq 0, \end{cases}$$

8:       update position of  $(x_i, y_i)$  by  $(x_i^{k+1}, y_i^{k+1}) = (x_i, y_i) - \alpha_i * g_i / \|g_i\|$ 
9:       break
10:    end if
11:  end for
12:  Calculate boundary loss  $\ell_b(x_i, y_i)$  and get subgradient  $g_i$  of  $\ell_b(x_i, y_i)$  by automatic differentiation.
13:  Calculate step by
           
$$\alpha_i = \begin{cases} x_i - (W - \frac{w_i}{2}) & \text{if } \frac{\partial \ell_b}{\partial x} > 0, \\ \frac{w_i}{2} - x_i & \text{if } \frac{\partial \ell_b}{\partial x} < 0, \\ y_i - (H - \frac{h_i}{2}) & \text{if } \frac{\partial \ell_b}{\partial y} > 0, \\ \frac{h_i}{2} - y_i & \text{if } \frac{\partial \ell_b}{\partial y} < 0. \end{cases}$$

14:  update position of  $(x_i, y_i)$  by  $(x_i^{k+1}, y_i^{k+1}) = (x_i, y_i) - \alpha_i * g_i$ 
15: end for

```

Table 1 GSRC benchmark circuit standards

circuit	module	terminal	net	pin	$\mathbf{W} \times \mathbf{H}$	Die-Area(mm ²)
n10	10	69	118	248	800 × 800	640000
n30	30	212	349	743	800 × 800	640000
n50	50	209	485	1050	800 × 800	640000
n100	100	334	885	1873	800 × 800	640000
n200	200	564	1585	3599	800 × 800	640000
n300	300	569	1893	4358	800 × 800	640000

Table 2 The experimental results of RBSM, GD, and ADAM methods in different circuits of the GSRC benchmark. Where lhpwl means the wirelength after legalization. In the RBSM and ADAM methods, the average field force coefficient $\alpha = 5$, the batch size is 1/5 of the total number of nets, and the initial value of parameter γ is 1000. In the GD method, γ is set to a constant of 1000.

Circuits	GSRC		RBSM			
	hpwl	overlap	hpwl	overlap	time(s)	lhpwl
n10	64299	0	56902	7206	7.48	56894
n30	179811	0	156761	1896	6.89	157261
n50	234281	0	199356	602	3.30	199236
n100	395719	0	328705	1470	5.78	328991
n200	738707	0	571720	2450	17.76	574778
n300	937608	0	694527	3634	36.12	698867.6

Circuits	GD			ADAM				
	hpwl	overlap	time(s)	lhpwl	hpwl	overlap	time(s)	lhpwl
n10	63959	82	0.45	63955	59631	29460	8.83	62240
n30	188770	612	0.40	188192	173825	35613	9.64	185765
n50	224062	1	0.63	224038	217210	42382	5.69	230797
n100	366449	1	0.92	366344	376827	20581	8.31	389947
n200	728562	0	2.16	728475	697857	19104	20.18	720499
n300	978937	60	3.76	978438	797910	71746	47.87	914895

achieve these objectives during the global placement phase. Consequently, our approach facilitates more efficient legalization and detailed placement in subsequent stages.

2. Compared to the GD algorithm without any enhanced techniques, the RBSM algorithm achieves a substantial reduction in wirelength. Notably, the wirelength after the legalization phase remains significantly shorter than that of the GD-based approach, underscoring the critical role of the enhancement techniques integrated into the RBSM algorithm.
3. When the gradient descent method in the RBSM algorithm is replaced with the ADAM optimizer, the algorithm’s performance deteriorates significantly, even falling below the performance of the GD method without enhancements. This indicates that gradient descent is more suitable for solving the rectified linear penalty

model of placement problems due to its stability and convergence properties in this context.

4. The proposed legalization algorithm not only eliminates overlap but also preserves the wirelength advantages achieved during placement. In some cases, it further reduces the wirelength. This result highlights the ability of the RBSM algorithm to maintain and even enhance placement quality, demonstrating its superiority in achieving short wirelength while ensuring overlap removal.

4.3 Analysis of our enhanced technique

In order to further illustrate the processing effectiveness of our optimization algorithm, we conducted a series of comparative experiments to assess the impact of four key enhancement techniques: degree-weighted sampling, adaptive parameter updating, mean-field force, and random disturbance on the algorithm respectively. The results presented are the average outcomes from five independent runs of each algorithm. For clarity, each comparison isolates the effect of a single enhancement by modifying only the corresponding component of the algorithm, allowing for a precise evaluation of its contribution.

Table 3 Comparative experiments on different enhancement techniques of RBSM method, with Original algorithm representing the results of RBSM method on corresponding circuits; Random batch represents the result of replacing weighted sampling with random sampling in the RBSM method (with the same sampling size); Fix gamma represents the result of using a fixed constant $\gamma = 10000$ instead of adaptive γ ; Without mean field force means that mean field force is not applied; Without random perturbation means the result without random perturbation.

Circuit	n100			n200			n300		
	hpwl	overlap	time	hpwl	overlap	time	hpwl	overlap	time
RBSM	328705	1470	5.78	571720	2450	17.66	694527	3634	36.12
Random batch	308666	3500	9.67	553329	4014	17.81	687753	5288	37.97
Fix gamma	368020	1691	2.52	642329	1349	6.34	871881	2229	16.18
No mean force	332958	2099	5.75	622479	1629	14.99	767695	3317	31.99
No perturbation	302856	3575	7.97	539778	7241	18.49	653182	10041	40.55

1) *Degree Weighted Sampling*: We compared random sampling with degree-weighted sampling. The experimental results for the n100, n200, and n300 circuits, under the same number of iteration steps, demonstrate that the overlap for random sampling is one to two times higher than that for degree-weighted sampling. This finding highlights that degree-weighted sampling enhances convergence performance by allocating more computational resources to critical nets, thereby accelerating the optimization process.

2) *Adaptive Parameter Adjustment*: The experimental results reveal that adaptive parameter updating significantly reduces wirelength compared to fixed-parameter algorithms. As the problem size increases, the performance gap becomes more pronounced. For instance, in the n100 circuit, the adaptive parameter adjustment reduces wirelength by 10%, and in the n300 circuit, it achieves a reduction of 20%. This

demonstrates that adaptive parameter selection provides stronger adaptability and optimization capability for circuit placement, enabling significant reductions in wirelength and overlap. However, it is important to note that the runtime of the adaptive parameter algorithm is approximately twice that of the fixed-parameter algorithm, indicating potential areas for future optimization.

3) *Mean Field Force*: As can be seen in the table, removing the mean field force from the algorithm results in a 1%, 8%, and 10% increase in wirelength for the n100, n200, and n300 circuits, respectively, compared to our full algorithm. This shows that adding the force of the aggregation effect can significantly improve the placement effect, and the effect becomes more and more significant with the increase of the problem scale.

4) *Random Disturbance*: Under a fixed number of iterations, incorporating random disturbance effectively reduces overlap. This is because random perturbations enable the algorithm to escape local minima, thereby accelerating convergence and improving overall optimization efficiency. This mechanism allows the algorithm to better explore the solution space, leading to improved placement quality.

These experimental results collectively demonstrate the importance and effectiveness of the proposed enhancements in improving the performance of the placement algorithm. Each component contributes uniquely to addressing specific challenges in circuit placement.

5 Conclusion

In this paper, we take a new perspective to solve the placement problem and transform it into a neural net training problem. A nonsmooth optimization model for VLSI global placement is proposed, with half-perimeter wirelength minimization and cell overlap elimination as the primary objectives and constraints. A penalty function model is established as a loss function, which can be formulated as a deep neural network with only ReLU layers without gradient vanishing and exploding issues. A stochastic subgradient method with operator splitting is proposed to solve the unconstrained nonsmooth optimization problem, and several optimization acceleration techniques are adopted to accelerate the convergence. Numerical experiments show that our model can effectively reduce HPWL and cell overlap on medium-scale data sets, and the obtained high-quality solutions can provide references for other imprecise algorithms. The current implementation of the proposed algorithm has some shortcomings in processing speed compared with other methods, its efficiency needs to be further improved for large-scale placement problems, which will be the focus of future research.

Acknowledgements

This work is partially supported by the National Key R&D Program of China (grant number 2021YFA1003601), the Strategic Priority Research Program of Chinese Academy of Sciences (No. XDA27010101), and the National Natural Science Foundation of China (grant number 12021001, 12171467).

Ethics declarations

Conflict of interest

The authors have no conflict of interest to declare that are relevant to the content of this article.

Data availability statement

The authors confirm that the data supporting the findings of this study are available within the article [15] and its supplementary materials.

Appendix A Visual placement effect display

Here we present some figures to display visual placement effects. Fig. A1–Fig. A6 show the comparison of placement effects. Fig. A7 shows the legalization results.

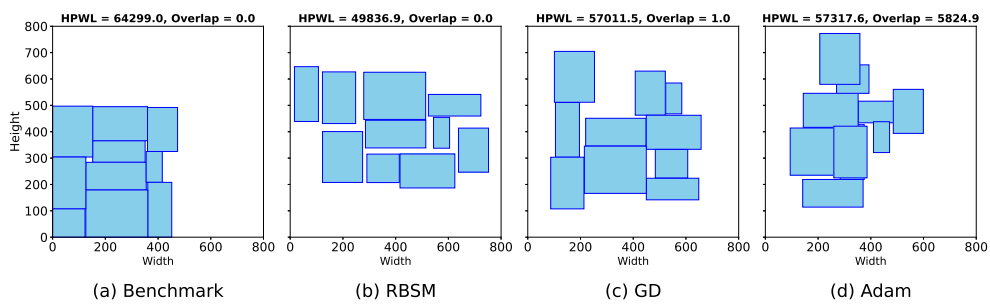


Fig. A1 Placement comparison for $n = 10$ using different methods

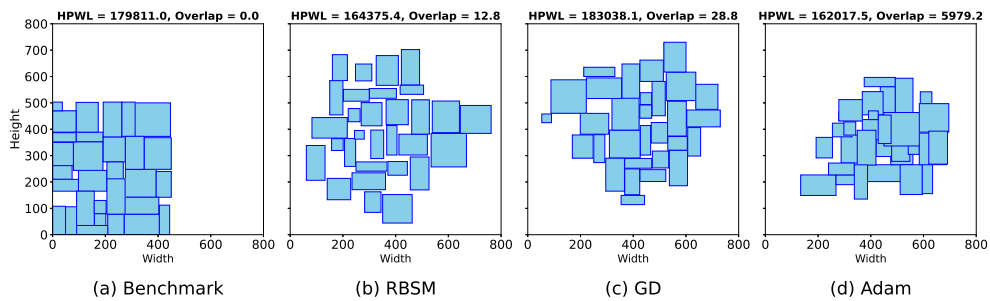


Fig. A2 Placement comparison for $n = 30$ using different methods

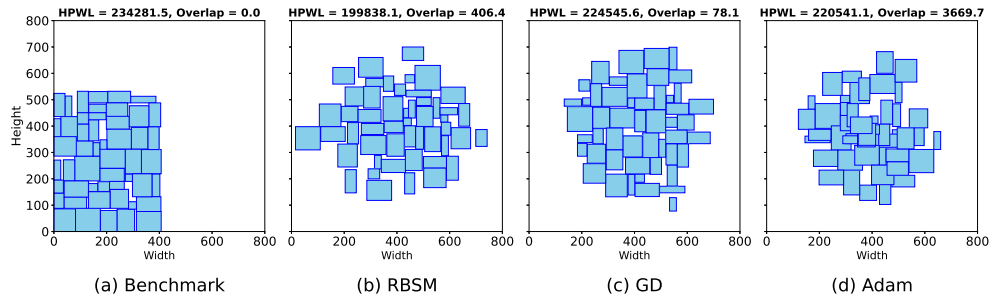


Fig. A3 Placement comparison for $n = 50$ using different methods

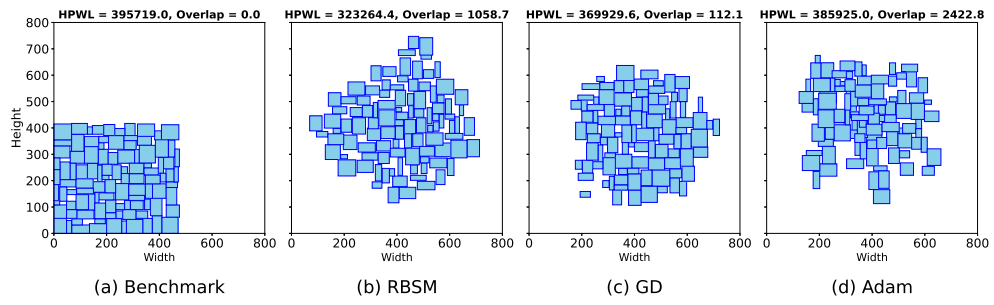


Fig. A4 Placement comparison for $n = 100$ using different methods

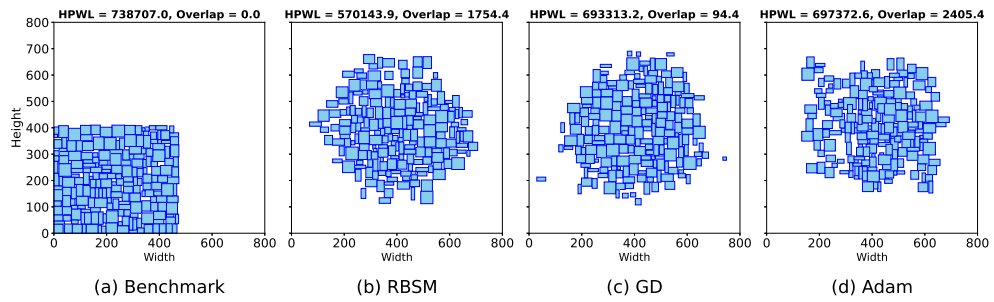


Fig. A5 Placement comparison for $n = 200$ using different methods

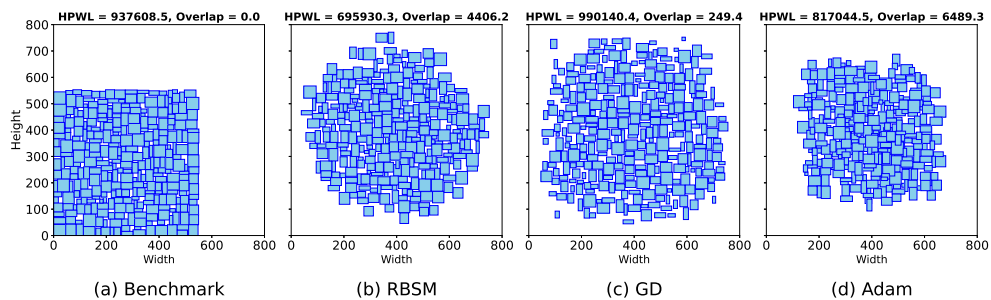


Fig. A6 Placement comparison for $n = 300$ using different methods

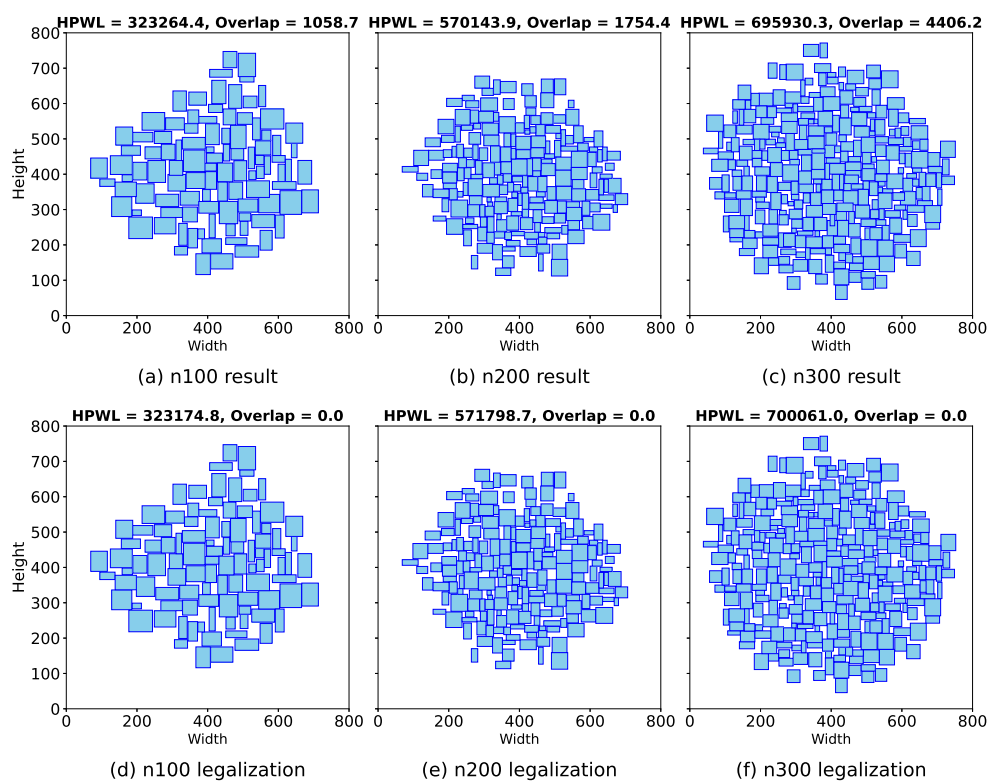


Fig. A7 Comparison between the results of RBSM method and the regularization results

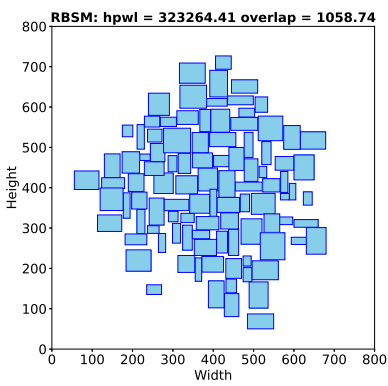
References

- [1] Alpert, C.J., Mehta, D.P., Sapatnekar, S.S.: Handbook of Algorithms for Physical Design Automation. CRC Press, New York (2008). <https://doi.org/10.1201/9781420013481>

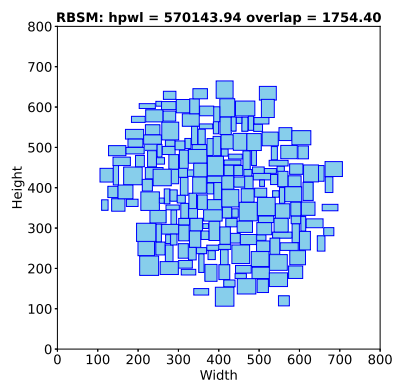
- [2] Kahng, A.B., Lienig, J., Markov, I.L., Hu, J.: VLSI Physical Design: From Graph Partitioning to Timing Closure. Springer, Heidelberg, Germany (2011). <https://doi.org/10.1007/978-90-481-9591-6>
- [3] Sechen, C.: VLSI Placement and Global Routing Using Simulated Annealing vol. 54. Springer, New York, NY (2012)
- [4] LaSalle, D., Karypis, G.: Multi-threaded graph partitioning. In: 2013 IEEE 27th International Symposium on Parallel and Distributed Processing, pp. 225–236 (2013). <https://doi.org/10.1109/IPDPS.2013.70> . IEEE
- [5] Viswanathan, N., Pan, M., Chu, C.: FastPlace 3.0: A fast multilevel quadratic placement algorithm with placement congestion control. In: 2007 Asia and South Pacific Design Automation Conference, pp. 135–140 (2007). <https://doi.org/10.1109/ASPDAC.2007.357975> . IEEE
- [6] Caldwell, A.E., Kahng, A.B., Markov, I.L.: Optimal partitioners and end-case placers for standard-cell layout. In: Proceedings of the 1999 International Symposium on Physical Design, pp. 90–96 (1999). <https://doi.org/10.1109/43.892854>
- [7] Huang, Z., Li, X., Zhu, W.: Optimization models and algorithms for placement of very large scale integrated circuits. Operations Research Transactions **25**(03), 15–36 (2021) <https://doi.org/10.15960/j.cnki.issn.1007-6093.2021.03.002>
- [8] Chan, T., Cong, J., Sze, K.: Multilevel generalized force-directed method for circuit placement. In: Proceedings of the 2005 International Symposium on Physical Design, pp. 185–192 (2005). <https://doi.org/10.1109/IPDPS.2013.70>
- [9] Naylor, W.C., Donnelly, R., Sha, L.: Non-linear optimization system and method for wire length and delay optimization for an automatic electric circuit placer. Google Patents. US Patent 6,301,693 (2001). <https://doi.org/US6301693>
- [10] Hsu, M.-K., Chang, Y.-W., Balabanov, V.: TSV-aware analytical placement for 3d IC designs. In: Proceedings of the 48th Design Automation Conference, pp. 664–669 (2011)
- [11] Chen, T.-C., Jiang, Z.-W., Hsu, T.-C., Chen, H.-C., Chang, Y.-W.: NTUplace3: An analytical placer for large-scale mixed-size designs with preplaced blocks and density constraints. IEEE Trans. Comput. Aided Des. Integr. Circuits Syst. **27**(7), 1228–1240 (2008) <https://doi.org/10.1109/TCAD.2008.923063>
- [12] Zhu, W., Chen, J., Peng, Z., Fan, G.: Nonsmooth optimization method for VLSI global placement. IEEE Trans. Comput.-Aided Des. Integr. Circuits Syst. **34**(4), 642–655 (2015) <https://doi.org/10.1109/TCAD.2015.2394484>
- [13] Sun, J., Cheng, H., Wu, J., Zhu, Z., Chen, Y.: Floorplanning of VLSI by mixed-variable optimization. In: International Symposium on Intelligence Computation

and Applications, pp. 137–151 (2023). Springer

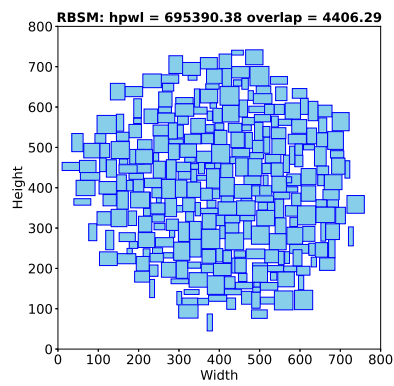
- [14] Paszke, A., Gross, S., Massa, F., Lerer, A., Bradbury, J., Chanan, G., Killeen, T., Lin, Z., Gimelshein, N., Antiga, L., et al.: Pytorch: An imperative style, high-performance deep learning library. *Adv. Neural Inf. Process. Syst.* **32** (2019) <https://doi.org/10.48550/arXiv.1912.01703>
- [15] Salama, H.F., Reeves, D.S., Viniotis, Y.: GSRC floorplan benchmarks (1997)
- [16] Chang, Y.-W., Jiang, Z.-W., Chen, T.-C.: Essential issues in analytical placement algorithms. *IPSJ Trans. Syst. LSI Des. Methodol.* **2**, 145–166 (2009) <https://doi.org/10.2197/ipsjtsldm.2.145>
- [17] Lin, Y., Dhar, S., Li, W., Ren, H., Khailany, B., Pan, D.Z.: Dreamplace: Deep learning toolkit-enabled GPU acceleration for modern VLSI placement. In: *Proceedings of the 56th Annual Design Automation Conference 2019*, pp. 1–6 (2019). <https://doi.org/10.1109/TCAD.2020.3003843>
- [18] Jin, S., Li, L., Sun, Y.: On the random batch method for second order interacting particle systems. *Multiscale Model. Simul.* **20**(2), 741–768 (2022) <https://doi.org/10.1137/20M1383069>
- [19] Lu, J., Chen, P., Chang, C.-C., Sha, L., Huang, D.J.-H., Teng, C.-C., Cheng, C.-K.: ePlace: Electrostatics based placement using Nesterov’s method. In: *Proceedings of the 51st Annual Design Automation Conference*, pp. 1–6 (2014). <https://doi.org/10.1145/2593069.2593216>
- [20] Zhou, T., Ren, J., Medo, M., Zhang, Y.-C.: Bipartite network projection and personal recommendation. *Phys. Rev. E Stat. Nonlin. Soft Matter Phys.* **76**(4), 046115 (2007) <https://doi.org/10.1103/PhysRevE.76.046115>
- [21] Weiss, P.: L’hypothèse du champ moléculaire et la propriété ferromagnétique. *J. Phys. Theor. Appl.* **6**(1), 661–690 (1907) <https://doi.org/10.1051/jphysap:019070060066100>
- [22] Xiao, S., Wang, H., Wang, W., Huang, Z., Zhou, X., Xu, M.: Artificial bee colony algorithm based on adaptive neighborhood search and gaussian perturbation. *Appl. Soft Comput.* **100**, 106955 (2021) <https://doi.org/10.1016/j.asoc.2020.106955>
- [23] Nocedal, J., Wright, S.J.: *Numerical Optimization*. Springer, New York, NY (1999). <https://doi.org/10.1007/978-0-387-40065-5>
- [24] Kingma, D.P., Ba, J.: Adam: a method for stochastic optimization. *arXiv:1412.6980 [cs]* (2014). Accessed 2018-04-24



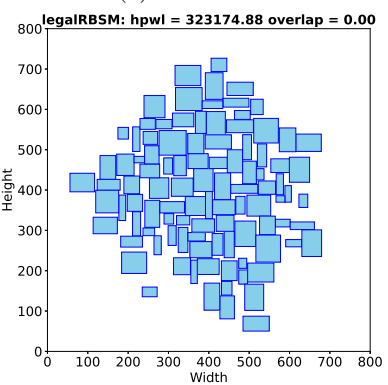
(a) n100 result



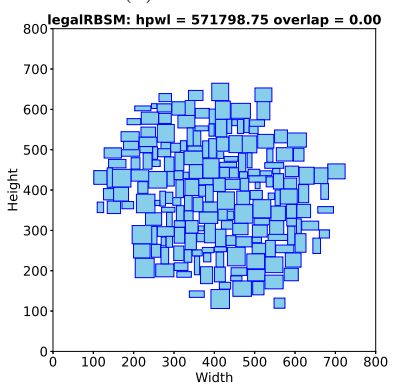
(b) n200 result



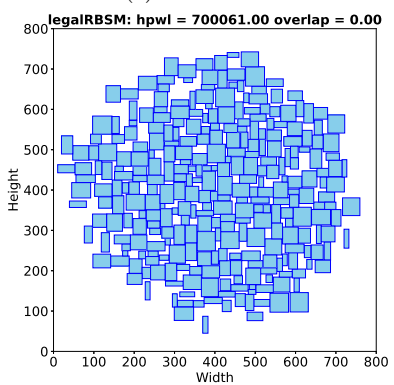
(c) n300 result



(d) n100 legalization



(e) n200 legalization



(f) n300 legalization